Processing-Microstructure-Properties Correlation of Ultrasensitive Gas Sensors Produced by Electrospinning

Osnat Landau,[†] Avner Rothschild,[†,*] and Eyal Zussman[‡]

Department of Materials Engineering and Department of Mechanical Engineering, Technion−Israel Institute of Technology, Haifa 32000, Israel

Received September 15, 2008
Revised Manuscript Received November 25, 2008

In recent years, significant progress has been achieved in developing highly sensitive metal-oxide gas sensors using novel one-dimensional (1D) and quasi-1D nanostructured architectures.[1] Among the different strategies for producing such sensors, electrospinning offers several advantages including ease of fabrication and versatility.[2] Recent reports on nanocrystalline TiO_2[3] and SnO_2[4] gas sensors produced by electrospinning demonstrate excellent performance in terms of gas sensitivity, reversibility, and response time. These merits and in particular the exceptional sensitivity of electrospun sensors were attributed to their nanostructured fibrillar morphology,[3a] illustrating that the gas sensing properties of electrospun materials are closely tied to their microstructure, similar to their 3D thick film counterparts.[5] Therefore, careful optimization of the electrospinning process parameters and subsequent thermal treatments is essential to achieve high performance. In this work, we report on the processing-microstructure-properties correlation of nanostructured TiO_2 gas sensors produced by electrospinning of composite polymer/titanium oxide fibers followed by thermal compression (hot pressing) and calcination. Process parameters were varied systematically and their effect on the resultant morphologies and gas sensing properties were examined as described in the following. Careful optimization of processing conditions resulted in mesoporous TiO_2 layers displaying ultrahigh sensitivity toward NO_2 and CO gases.

The electrospun solution comprised poly(vinyl acetate) (PVAc, MW = 500 000 g/mol, Aldrich) dissolved in 3.75 mL of dimethylformamide (DMF) (AR, Frutarom) onto which 0.6 g of titanium(IV) propoxide (98% pure, Aldrich) and 0.24 g of acetic acid (AA) were added. The latter catalyzes the precipitation into the anatase TiO_2 phase.[6] The PVAc weight was varied between 0.1 and 0.6 g to obtain polymer concentrations, $W_{PVAc}/(W_{PVAc} + W_{DMF} + W_{Ti(IV)} + W_{AA})$, between 2 and 12 wt %, respectively, in order to examine the effect on microstructure. The solution was loaded into a syringe and connected to a high-voltage power supply. An electric field of 1.5 kV/cm was applied between the stainless steel orifice (inner diameter = 450 μm) and the grounded collector 10 cm below the orifice. The precursor solution was electrospun at room temperature on wax paper or Si wafers placed on a rotating horizontal collector spinning at 100 rpm. The amount of electrospun solution was 1 mL and the flow rate was 1.5 mL/h. The electrospun layers were dried in vacuum for 48 h (at room temperature) to remove the organic solvents. The layers had a thickness of about 80 μm after drying. Subsequently, the electrospun layers that were deposited on wax papers were cut into 8 mm × 13 mm pieces and hot pressed on Si/SiN_x substrates fitted with interdigitated Au electrode arrays (5 mm long and 20 μm wide Au fingers spaced 20 μm apart).

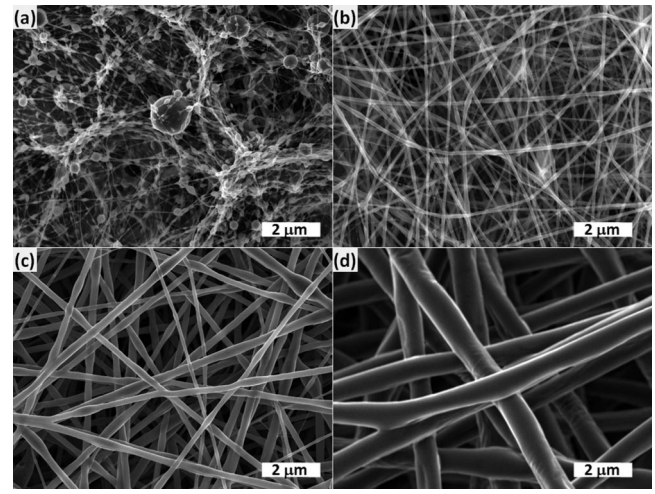

Figure 1. SEM micrographs of electrospun layers with polymer concentrations of (a) 2, (b) 5, (c) 8, and (d) 12 wt % following electrospinning and vacuum drying and prior to thermal treatments.

Figure 1 shows the morphology of the electrospun layers obtained with different polymer concentrations. At low concentrations (≤2 wt %) they comprised network of small beads interconnected by thin fibers (Figure 1a). This morphology can be ascribed to capillary instability in low viscous solutions.[7] At higher concentrations (≥5 wt %), the beads disappeared and the fibers became continuous and quite homogeneous. Their diameter increased with increasing polymer concentrations: 120 ± 20, 270 ± 70, and 850 ± 110 nm for 5, 8, and 12 wt %, respectively.

Following the electrospinning process, the layers were vaccuum-dried (48 h) and subsequently a thermal compression step was carried out to improve the adhesion between the electrospun layers and the substrates. The layers were

* Corresponding author. E-mail: avnerrot@technion.ac.il.
† Department of Material Engineering, Technion.
‡ Department of Mechanical Engineering, Technion.

(1) Comini, E. *Anal. Chim. Acta* **2006**, *568*, 28.
(2) (a) Reneker, D. H.; Yarin, A. L.; Zussman, E. *Adv. Appl. Mech.* **2007**, *41*, 43. (b) Ramaseshan, R.; Sundarrajan, S.; Jose, R.; Ramakrishna, S. *J. Appl. Phys.* **2007**, *102*, 111101.
(3) (a) Kim, I.-D.; Rothschild, A.; Lee, B. H.; Kim, Y. D.; Jo, S. M.; Tuller, H. L. *Nano Lett.* **2006**, *6*, 2009. (b) Li, Z.; Zhang, H.; Zheng, W.; Wang, W.; Huang, H.; Wang, C; MacDiarmid, A. G.; Wei, Y. *J. Am. Chem. Soc.* **2008**, *130*, 5036.
(4) (a) Yang, A.; Tao, X.; Wang, R.; Lee, S.; Surya, C. *Appl. Phys. Lett.* **2007**, *91*, 133110. (b) Zhang, Y.; He, X.; Li, J.; Miao, Z.; Huang, F. *Sens. Actuators, B* **2008**, *132*, 67.
(5) (a) Williams, D. E.; Pratt, K. F. *Sens. Actuators, B* **2000**, *70*, 214. (b) Barsan, N.; Weimar, U. *J. Electroceramics* **2001**, *7*, 143. (c) Shimizu, Y.; Hyodo, T.; Egashira, M. *Catal. Surv. Asia* **2004**, *8*, 127. (d) Korotcenkov, G. *Mater. Sci. Eng., R* **2008**, *61*, 1.
(6) Parra, R.; Goes, M. S.; Castro, M. S.; Longo, R.; Bueno, P. R.; Varela, J. A. *Chem. Mater.* **2008**, *20*, 143.
(7) Theron, S. A.; Zussman, E.; Yarin, A. L. *Polymer* **2004**, *45*, 2017.

10.1021/cm802498c CCC: $40.75
Published on Web 12/16/2008

pressed onto the substrate between stainless steel dies heated to 90 °C. Two-millimeter-thick Teflon disks were inserted between the layer and press dies to apply a uniform pressure and prevent sticking. A pressure ranging between 3 and 800 kPa was applied for 10 min. The thermal compression was carried out above the glass transition temperature of PVAc (~30 °C) and below the temperature at which the electrospun mats started to lose weight (120 °C) based on thermogravimetric analysis (TGA). We did not observe notable variations in morphology as function of the applied pressure and a pressure of 200 kPa was selected for subsequent experiments. The layers were compressed quite significantly but otherwise they maintained their as-spun morphology.

Following the thermal compression step, the samples were calcined in air to remove the organic compounds and crystallize the Ti(IV) precursor to TiO_2. The temperature profile comprised three intermediate steps at 280, 350, and 420 °C, followed by final annealing step at 450, 500, 750, or 800 °C. This profile was designed, based on TGA measurements, in order to gradually remove the organic components. Each step took 5 h and the ramp rate was 5 °C/min. The layer shrank to about 10 μm following the thermal compression and calcination steps. The resulting morphology, microstructure, and chemical composition were examined using SEM, XRD, FTIR, and XPS. In accord with the TGA measurements that showed that the weight loss occurred at temperatures below 420 °C, no characteristic peaks of any of the organic components in the electrospun solution were observed in the FTIR spectra of the calcined specimens. Likewise, no impurities (other than C, which is a common surface contaminant often observed in XPS) were observed in their XPS spectra. Following calcination at 450 °C the layers crystallized to polycrystalline TiO_2 anatase and no remnants of an amorphous phase were observed by XRD. The anatase phase remained stable and did not transform to rutile up to 800 °C.

In the bulk form, anatase is a metastable polymorph of TiO_2 that irreversibly transforms to rutile at several hundred degrees Celsius (the transformation is kinetically limited and the transition temperature varies between ca. 400 and 900 °C depending of the grain size, impurity content, and other parameters), but in nanosized titania, anatase is often observed as the predominant phase at temperatures as high as 850 °C.[8] The stabilization of anatase in nanosized titania has been explained by taking account of the competition between the contributions of the formation enthalpy and surface energy to the free energy of the respective phases.[9] Thus, the small surface energy of anatase (~0.4 J/m^2) compared to rutile (~2.2 J/m^2) leads to a crossover in thermodynamic stability at the nanoscale because of the high surface-to-volume ratio of nanocrystallites.[10]

Figure 2 shows the morphologies obtained following calcination at 500 °C for the same polymer concentrations as in Figure 1. The highest porosity and smallest grain size were found in the richest electrospun solution (12 wt %). Because high porosity and small grain size enhance gas sensitivity,[5] this composition was identified as the most promising candidate for gas sensing applications and was further investigated to determine the optimal calcination temperature. Calcination at 450 °C, the minimum temperature necessary to remove the organic compounds in the electrospun layer, yielded mesoporous morphology with ~10% porosity (evaluated from the SEM micrographs) and typical particle size of 29 ± 5 nm. Calcination at 750 °C increased the porosity to ~40% and the particle size to 42 ± 5 nm. Because both porosity and particle size increase with increasing calcination temperatures, it is difficult to determine a priori the optimal calcination conditions for achieving the maximum sensitivity. A posteriori, the sensitivity was found to be consistently higher for samples calcined at 750 °C than for those calcined at 450 °C. We note that in both cases, the grain size is smaller than twice the Debye length (ca. 20−25 nm), a necessary condition to obtain high sensitivity.[11]

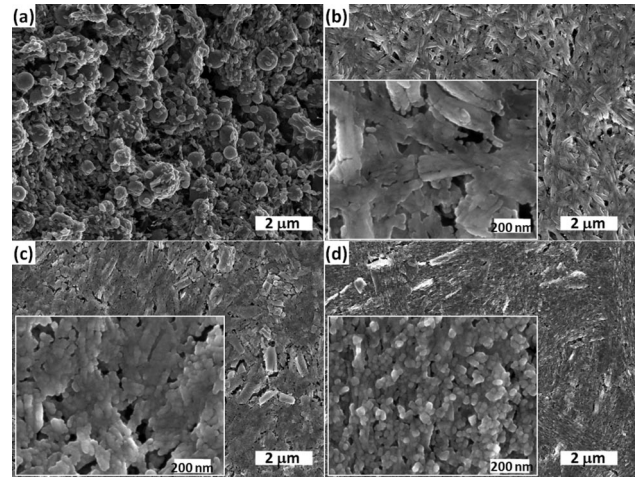

Figure 2. SEM micrographs of electrospun layers with polymer concentrations of (a) 2, (b) 5, (c) 8, and (d) 12 wt % following hot pressing and calcination at 500 °C.

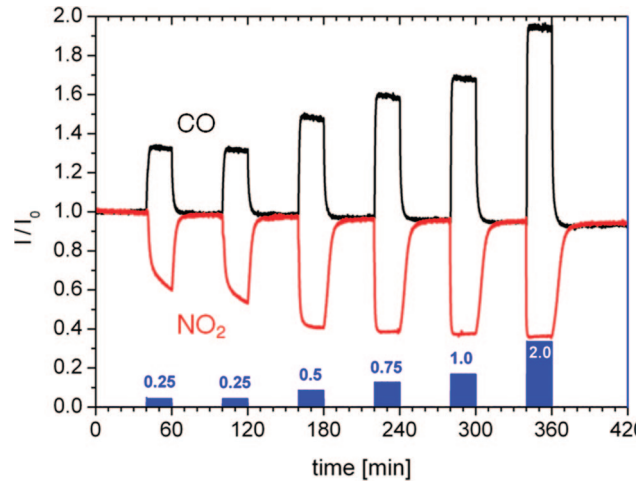

Figure 3. Electrical response of electrospun TiO_2 sensor (12 wt %, calcined at 750 °C) upon cyclic exposure to CO or NO_2 pulses at 400 °C. The gas exposure profile (concentration in parts per million) is indicated at the bottom.

(8) (a) So, W. W.; Park, S. B.; Kim, K. J.; Shin, C. H.; Moon, S. J. *J. Mater. Sci.* **2001**, *36*, 4299. (b) Li, W.; Ni, C.; Lin, H.; Huang, C. P.; Ismat Shah, S. *J. Appl. Phys.* **2004**, *96*, 6663.
(9) (a) Grib, A. A.; Banfield, J. F. *Am. Mineral.* **1997**, *82*, 717. (b) Zhang, H.; Banfield, J. F. *J. Mater. Chem.* **1998**, *8*, 2073.
(10) Ranade, M. R.; Navrotsky, A.; Zhang, H. Z.;.; Banfield, J. F.; Elder, S. H.; Zaban, A.; Borse, P. H.; Kulkarni, S. K.; Doran, G. S.; Whitfield, H. J. *Proc. Natl. Acad. Sci. U.S.A.* **2002**, *99*, 6476.

Table 1. Gas Sensing Characteristics at 300 and 400 °C

	CO						NO_2					
	I/I_0		response time (t_{90}) (min)		recovery time (t_{90}) (min)		I_0/I		response time (t_{90}) (min)		recovery time (t_{90}) (min)	
concentration (ppb)	300 °C	400 °C	300 °C	400 °C	300 °C	400 °C	300 °C	400 °C	300 °C	400 °C	300 °C	400 °C
50	1.05	1.03	3.8	4.5	1.1	2.0	5.1	1.3	4.6	4.9	4.4	5.3
100	1.07	1.06	2.6	2.1	1.3	0.8	15.9	1.9	2.4	4.2	5.2	4.1
150	1.10	1.11	2.2	2.0	1.3	1.3	51.7	2.6	1.4	3.9	6.0	4.4
200	1.11	1.14	2.2	1.8	1.3	1.3	70.3	3.1	1.1	1.9	6.4	5.4
250	1.15	1.17	2.4	1.5	1.6	1.8	74.3	3.3	0.8	1.4	4.4	4.8

Figure 3 shows the electrical response of an electrospun TiO_2 sensor prepared from a 12 wt % solution and calcined at 750 °C upon cyclic exposure to CO or NO_2 pulses in dry air at 400 °C. The response is presented as the normalized DC current passing through the layer under a bias of 50 mV with respect to the baseline current ($I_0 \sim 900$ pA) in dry air at the beginning of the measurement. The gas exposure profile (concentration in parts per million) is indicated at the bottom of the graph. The conductivity increases upon exposure to CO and decreases for NO_2, in line with the typical response on n-type semiconducting metal-oxides exposed to reducing and oxidizing species, respectively.[12] The response is significantly higher than the white noise of the baseline signal (~0.8%) for all the exposure levels. Furthermore, it is fully reversible with response time and recovery time of several min. Similar results were obtained also at lower gas concentrations down to 50 ppb as summarized in Table 1. The sensor was more sensitive at 300 °C than at 400 °C, demonstrating exceptional sensitivity toward NO_2 displaying a change of 405% in the sensor's resistance on exposure to 50 ppb of NO_2. By extrapolating the results to lower gas concentrations we estimate the detection limit to be ~5 ppb for NO_2 and ~20 ppb for CO (both at 300 °C). These results favorably compare with the highest sensitivity values reported in the open literature for metal-oxide gas sensors in general[13] and TiO_2-based sensors in particular.[3]

In summary, the microstructure evolution of electrospun TiO_2 layers was investigated and processing conditions were optimized to achieve highly porous nanostructures tailored for ultrahigh gas sensitivity. These sensors demonstarted the ability to detect traces of NO_2 and CO in air well below the environmental standards for these gases,[14] suggesting potential applications in environmental monitoring.

Acknowledgment. This work was partially supported by the Russell Berrie Nanotechnology Institute (RBNI) of the Technion and by the Jewish Communities of Germany Research Fund. The authors thank Dr. Il-Doo Kim of the Korea Institute of Science and Technology (KIST) for providing the interdigitated Si substrates on which the TiO_2 sensors were prepared.

CM802498C

(11) Rothschild, A.; Komem, Y. *J. Appl. Phys.* **2004**, *95*, 6374.
(12) Williams, D. E. *Sens. Actuators, B* **1999**, *57*, 1.
(13) (a) Yamazoe, N. *Sens. Actuators, B* **2005**, *108*, 2. (b) Tamaki, J. *Sens. Lett.* **2005**, *3*, 89. (c) Zhang, D.; Liu, Z.; Li, C.; Tang, T.; Liu, X.; Han, S.; Lei, B.; Zhou, C. *Nano Lett.* **2004**, *4*, 1919.
(14) *National Ambient Air Quality Standards (NAAQS)*; U.S. Environmental Protection Agency: Washington, D.C.; available at http://www.epa.gov/air/criteria.html.